Chinese Journal of Natural Medicines

Lingguizhugan Decoction improves chronic heart failure by synergistically modulating β1-AR/Gs/GRKs/β-arrestin signaling bias

Shuting Guo, Lei Xia, Songru Yang, Yueyang Liang, Xiaoli Shan, Pei Zhao, Wei Guo, Chen Zhang, Ming Xu, Ning Sun, Rong Lu, Huihua Chen

Citation: Shuting Guo, Lei Xia, Songru Yang, Yueyang Liang, Xiaoli Shan, Pei Zhao, Wei Guo, Chen Zhang, Ming Xu, Ning Sun, Rong Lu, Huihua Chen, Lingguizhugan Decoction improves chronic heart failure by synergistically modulating β1-AR/Gs/GRKs/β-arrestin signaling bias, Chinese Journal of Natural Medicines, 2025, 23(5), 560-571. doi: 10.1016/S1875-5364(25)60863-6.

View online: https://doi.org/10.1016/S1875-5364(25)60863-6

Related articles that may interest you

Qi-Tai-Suan, an oleanolic acid derivative, ameliorates ischemic heart failure *via* suppression of cardiac apoptosis, inflammation and fibrosis

Chinese Journal of Natural Medicines. 2022, 20(6), 432-442 https://doi.org/10.1016/S1875-5364(22)60156-0

Shengmaisan combined with Liuwei Dihuang Decoction alleviates chronic intermittent hypoxia-induced cognitive impairment by activating the EPO/EPOR/JAK2 signaling pathway

Chinese Journal of Natural Medicines. 2024, 22(5), 426-440 https://doi.org/10.1016/S1875-5364(24)60640-0

Protective effects of Wuwei Xiaodu Drink against chronic osteomyelitis through $Foxp3^{+}CD25^{+}CD4^{+}$ Treg cells *via* the IL-2/STAT5 signaling pathway

Chinese Journal of Natural Medicines. 2022, 20(3), 185-193 https://doi.org/10.1016/S1875-5364(22)60146-8

Effects of chitooligosaccharide-zinc on the ovarian function of mice with premature ovarian failure *via* the SESN2/NRF2 signaling pathway

Chinese Journal of Natural Medicines. 2021, 19(10), 721-731 https://doi.org/10.1016/S1875-5364(21)60084-5

Compound Sophorae Decoction: treating ulcerative colitis by affecting multiple metabolic pathways

Chinese Journal of Natural Medicines. 2021, 19(4), 267-283 https://doi.org/10.1016/S1875-5364(21)60029-8

A systematic review of pharmacological activities, toxicological mechanisms and pharmacokinetic studies on *Aconitum* alkaloids

Chinese Journal of Natural Medicines. 2021, 19(7), 505-520 https://doi.org/10.1016/S1875-5364(21)60050-X

Wechat

Chinese Journal of Natural Medicines 23 (2025) 560-571

Contents lists available at ScienceDirect

Chinese Journal of Natural Medicines

journal homepage: www.cjnmcpu.com/

Original article

Lingguizhugan Decoction improves chronic heart failure by synergistically modulating β1-AR/Gs/GRKs/β-arrestin signaling bias

Shuting Guo[a,Δ], Lei Xia[a,Δ], Songru Yang[a], Yueyang Liang[a], Xiaoli Shan[a], Pei Zhao[a], Wei Guo[b], Chen Zhang[b], Ming Xu[b], Ning Sun[c], Rong Lu[a,*], Huihua Chen[a,*]

[a] *School of Traditional Chinese Medicine, Shanghai University of Traditional Chinese Medicine, Shanghai 200000, China*
[b] *School of Integrative Medicine, Shanghai University of Traditional Chinese Medicine, Shanghai 200000, China*
[c] *Wuxi School of Medicine, Jiangnan University, Wuxi 214000, China*

ARTICLE INFO

Article history:
Received 2 October 2024
Revised 24 November 2024
Accepted 4 December 2024
Available online 20 May 2025

Keywords:
Lingguizhugan Decoction
Chronic heart failure
Isoproterenol

ABSTRACT

Lingguizhugan Decoction (LGZG) demonstrates significant efficacy in treating various cardiovascular diseases clinically, yet its precise mechanism of action remains elusive. This study aimed to elucidate the potential mechanisms and effects of LGZG on isoproterenol (ISO) continuous stimulation-induced chronic heart failure (CHF) in mice, providing direct experimental evidence for further clinical applications. *In vivo*, continuous ISO infusion was administered to mice, and ventricular myocytes were utilized to explore LGZG's potential mechanism of action on the β1-adrenergic receptor (β1-AR)/Gs/G protein-coupled receptor kinases (GRKs)/β-arrestin signaling deflection system in the heart. The findings reveal that LGZG significantly reduced the messenger ribonucleic acid (mRNA) expression of hypertrophy-related biomarkers [atrial natriuretic peptide (ANP) and B-type natriuretic peptide (BNP)] and improved cardiac remodeling and left ventricular diastolic function in mice with ISO-induced CHF. Furthermore, LGZG inhibited the overactivation of Gs/cyclic adenosine monophosphate (cAMP)/protein kinase A (PKA) signaling and downregulated the downstream transcriptional activity of cAMP-response element binding protein (CREB) and the expression of the coactivator CBP/P300. Notably, LGZG downregulated the expression of β-arrestin1 and GRK 2/3/5 while upregulating the expression of β1-AR and β-arrestin2. These results suggest that LGZG inhibits Gs/cAMP/PKA signaling and β-arrestin/GRK-mediated desensitization and internalization of β1-AR, potentially exerting cardioprotective effects through the synergistic regulation of the β1-AR/Gs/GRKs/β-arrestin signaling deflection system *via* multiple pathways.

1. Introduction

Despite significant advancements in the prevention and treatment of chronic heart failure (CHF) over the past five decades, it has emerged as a leading cause of mortality, posing a substantial threat to human health due to its increasing morbidity and mortality rates. The pathogenesis of CHF is multifaceted, with overactivation of β1-adrenergic receptor (β1-AR)/Gs/protein kinase A (PKA) signaling being a primary pathogenic mechanism [1]. Consequently, β1-AR has become a crucial target for CHF treatment, and the widespread implementation of β1-AR blockers has significantly alleviated clinical symptoms and reduced mortality in CHF patients [2]. However, ligands can activate various downstream signaling pathways by inducing conformational changes in G-protein-coupled receptor (GPCR). β1-AR, a prototypical member of the GPCR superfamily, mediates the classical Gs-protein pathway and receptor internalization and desensitization, regulates apoptosis, and participates in pathological processes such as cardiac hypertrophy and failure through numerous β-arrestin-mediated signaling pathways [3]. Activated β1-AR elicits diverse, and sometimes opposing, biological effects through these different downstream signaling pathways. As a result, β1-AR blockers may inhibit both pathological signaling and receptor-mediated protective signaling, potentially leading to severe adverse effects. Promoting β1-AR bias towards interaction with protective signaling transducers, utilizing the differential activation of GPCRs and signaling bias, may be essential for the prevention and management of CHF [4,5].

Nevertheless, the screening process for biased ligands has been constrained due to the lack of two independent, non-overlapping signaling branches in β1-AR [6]. Furthermore, β1-AR exists in a constant equilibrium among multiple conformations, making it highly improbable for any single ligand to shift this equilibrium towards a specific signaling bias [4].

Traditional Chinese medicine (TCM), administered by experienced practitioners, enables the diagnosis and treatment of CHF using herbal formulations that effectively modulate multiple targets and pathways simultaneously [7]. Further investigation is warranted to determine whether Chinese herbal compounds exert a bidirectional regulatory effect on the intricate β1-AR/Gs/β-ar-

* Corresponding author.
E-mail addresses: lurong@shutcm.edu.cn (R. Lu); chenhuihua@shutcm.edu.cn (H. Chen)
Δ These authors contributed equally to this work.

https://doi.org/10.1016/S1875-5364(25)60863-6
Copyright © 2025, China Pharmaceutical University. Published by Elsevier B.V. All rights reserved.

restin signaling deflection system.

Lingguizhugan decoction (LGZG) is a traditional Chinese herbal formula originating from Zhang Zhong Jing's *Shanghan Zabing Lun* of the Han Dynasty [8]. In Chinese medicine, LGZG is believed to warm yang, alleviate fluid retention, strengthen the spleen, and eliminate dampness [9]. LGZG has demonstrated significant efficacy in the clinical treatment of various stages of cardiovascular diseases [10, 11]. The cardioprotective effects of LGZG involve multiple complex mechanisms. Studies have shown that LGZG and its active components regulate lipid metabolism, protein kinase B(AKT)/AMP-activated protein kinases (MAPKs), transforming growth factor-β1/Smads, and other signaling pathways [12–14]. This regulation may potentially reverse the pathological progression of cardiac hypertrophy, leading to heart failure. Additionally, LGZG has been found to significantly inhibit the overexpression of neuroendocrine cytokines, including renin-angiotensin–aldosterone system-related factors, tumor necrosis factor (TNF)-α, and nuclear factor-κB (NF-κB) [15]. However, its specific effects on CHF development and mechanism of action remain to be fully elucidated. Research has demonstrated that β-arrestin is a crucial regulator of β1-AR signaling bias and functions as a scaffolding protein to modulate various downstream intracellular signaling pathways including AMPKs, AKT, extracellular signal-regulated kinase (ERK), c-Jun N-terminal kinase (JNK), and NF-κB [16]. The activation of β-AR signaling bias by β-arrestin is a key pathological mechanism in CHF. Therefore, in contrast to previous studies, this research examines the upstream mechanisms and cardioprotective effects of LGZG by focusing on the regulation of Gs/β-arrestin-mediated β-AR signaling bias signaling bias.

2. Materials and methods

2.1. Preparation of LGZG

The herbal components of LGZG were sourced from Shanghai WanshiCheng Pharmaceutical, Ltd. (Shanghai, China) (Table 1), with all ingredients authenticated by the School of Pharmacy, Shanghai University of Chinese Medicine (Shanghai, China). Plant names were verified using http://mpns.kew.org. Granule preparation adhered to the Technical Requirements for Quality Control and Standard Preparation of Chinese Medicine Formula Granules, as mandated by the National Medical Products Administration of China. Following the prescribed ratio, 924 g of Chinese herbal medicine underwent two decoction processes: an initial 1-hour boil with eight times the water volume, followed by a 0.5-hour boil with six times the water volume. The combined decoction was filtered through an 80-mesh sieve and concentrated (70–80 °C) to yield 400–500 g of extract (1.12–1.15 g/cm^3). Spray drying without dextrin (entry air temperature, ≤ 165 °C; exit air temperature, 90–110 °C) produced approximately 130 g of dry powder, which was then dry-granulated (squeezing pressure, 15 MPa; extrusion speed, ≤ 35 rad/min) to obtain approximately 130 g of LGZG Granules (particle moisture ≤ 6%). To ensure LGZG quality and stability, high-performance liquid chromatography was employed to detect key medicinal components (chlorogenic acid, trans-cinnamic acid, liquiritin, and linoleic acid). The concentrations were determined as follows: chlorogenic acid, 28.2825 μg·mL^{-1}; trans-cinnamic acid, 54.7396 μg·mL^{-1}; liquiritin, 80.3768 μg·mL^{-1}; and linoleic acid, 3.0727 μg·mL^{-1}. Fig. 1 illustrates the chemical structures and chromatograms.

Prior to treatment, the following formula was utilized to determine the appropriate gavage dose for mice based on the equivalent human dose, according to surface area: mouse dose (g·kg·d^{-1}) = human dose (8 g·60 kg·d^{-1}) × 9.01. LGZG was dissolved in 0.9% sodium chloride to prepare a solution of 0.075 g·mL^{-1}. This solution was administered at doses of 1.2 and 2.4 g·kg·d^{-1}. For *in vitro* experiments, double distilled water (ddH_2O) was used to perform a gradient dilution of LGZG, ensuring that the osmolarity was comparable to that of the corresponding medium. The pH was adjusted to 7.4, after which the solution underwent centrifugation at 3000 r·min^{-1} for 30 min, followed by filtration through a 0.22-μm filtration system to remove bacteria, before preparation for use.

2.2. Animal manipulation

This study was approved by the Animal Care and Use Committee of Shanghai University of Traditional Chinese Medicine (SCXK 2016-0011) and conducted in accordance with the Guide for the Care and Use of Laboratory Animals. Adult male (C57BL/6J; weight, 20–23 g; age, 7 weeks) and neonatal (C57BL/6J) mice were obtained from the Shanghai Experimental Animal Center (Shanghai, China). The animals were housed at 22 ± 2 °C with a 12-h light/dark cycle and provided ad libitum access to standard diet and water for 1 week prior to the experiment. A model of pathological cardiac hypertrophy was established as previously described [17]. In brief, isoproterenol (ISO) (40 mg·kg·day^{-1}, ISO group) or vehicle (saline, sham group) was subcutaneously infused into the mice using mini-osmotic pumps (Alzet model 1002; Durect, Cupertino, CA, USA) for 4 weeks. The experimental mice were randomly assigned to five group : sham (n = 9), ISO (n = 8), atenolol treatment (n = 10, 10 mg·kg^{-1}), low-dose LGZG treatment (n = 10, 1.2 g·kg^{-1}), and high-dose LGZG treatment (n = 9, 2.4 g·kg^{-1}). The experiment concluded after 4 weeks of LGZG treatment.

2.3. H&E Staining, Masson's Trichrome Staining, and Sirius red staining

To evaluate morphological alterations in mouse hearts, tissue samples were fixed overnight in 4% paraformaldehyde, rinsed, and subsequently paraffin-embedded and sectioned. The sections were stained with hematoxylin and eosin. Following conventional deparaffinization of the paraffin sections, Masson's trichrome staining and Sirius-Red staining (both from KeyGEN BioTECH, Nanjing, China) were conducted to assess myocardial fibrosis. In Masson's trichrome staining, cardiomyocytes appeared red while collagen fibers stained blue. In Sirius red staining, collagen fibers were visualized as red. A blinded third party randomly selected myocardial interstitial and perivascular tissues for imaging under a 20x light microscope. Images were captured using a microscope and quantitatively analyzed using Image J software. The collagen volume fraction (CVF), encompassing both perivascular and interstitial collagen, was calculated as the ratio of collagen area to total area, expressed as a

Table 1 Components of Lingguizhugan Decoction.

Latin Name	Chinese name	Medicinal Part	Amount (g)	Origin of product	Production number
Wolfiporia cocos (F. A. Wolf) Ryvarden & Gilb.	Fuling	Dry sclerotium	24	Anhui, China	20220825-1
Cinnamomum cassia (L.) J. Presl	Guizhi	Dried branch	18	Guizhou, China	20220921-1
Atractylodes macrocephala Koidz.	Baizhu	Dried roots and rhizome	12	Anhui, China	20220430-1
Glycyrrhiza uralensis Fisch. exDC.	Gancao	Root and rhizome	12	Gansu, China	20220915-1

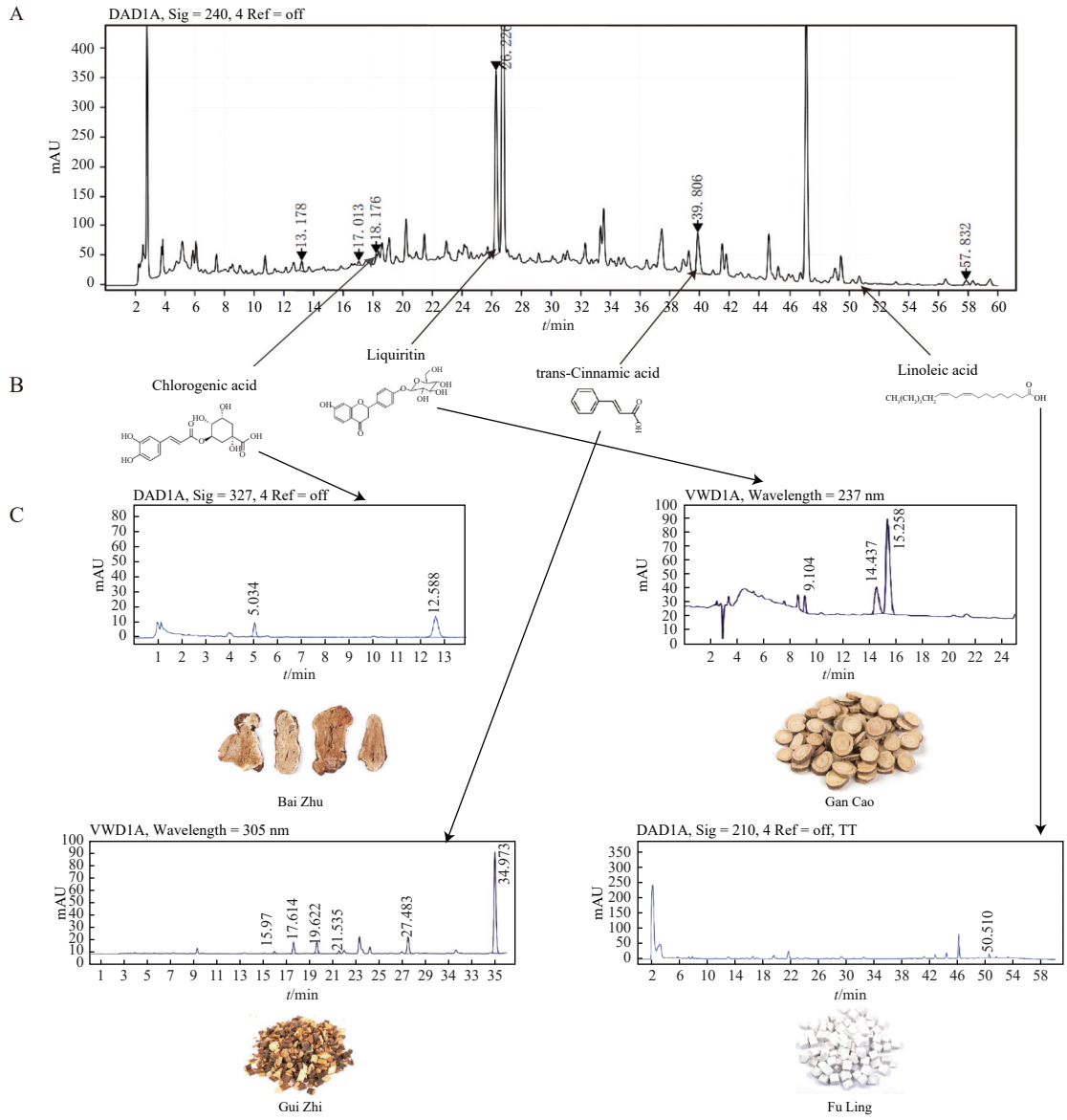

Fig. 1 Chemical structure and HPLC analysis of the main components in LGZG. (A) HPLC chromatogram of LGZG at 240 nm. (B) Chemical structures of chlorogenic acid, liquiritin, trans-cinnamic acid, and linoleic acid, are the main chemical components of LGZG. (C) HPLC chromatogram of chlorogenic acid, trans-cinnamic acid, liquiritin, and linoleic acid in the control herb was recorded at 240 nm. The images show the four components that makeup LGZG. HPLC, high-performance liquid chromatography; LGZG, Lingguizhugan Decoction.

percentage.

2.4. Neonatal mouse ventricular myocyte (NMVM) culture and treatment

NMVMs were isolated from neonatal mice within 24 hours of birth. Following decapitation, the hearts were extracted and rinsed. The ventricular tissue underwent digestion using a solution containing collagenase II and 0.25% trypsin (#25200072; Thermo Fisher Scientific, USA). Cells were then inoculated in six-well cell culture plates or confocal dishes, as previously described, and maintained in Dulbecco's Modified Eagle Medium/F12 medium (Gibco, USA) for 48 hours in a 5% CO_2 incubator at 37 °C.

For the *in vitro* experiments, LGZG underwent gradient dilution in ddH_2O. The osmolarity was evaluated to ensure comparability with the corresponding medium, and the pH was adjusted to 7.4. The solution was then filtered to remove bacteria and prepared for use. NMVMs were subsequently exposed to the following conditions for 48 h: Con, ISO (1 μmol·L^{-1}) group, ISO (1 μmol·L^{-1}) + LGZG (10^{-6} g·mL^{-1}), and ISO (1μmol·L^{-1}) + Atenolol (1 μmol·L^{-1}).

2.5. Adult mouse ventricular myocyte (AMVM) culture and treatment

AMVMs were isolated following a previously described protocol [18]. The mice were euthanized by deeply anesthetized with pentobarbital sodium (100 mg·kg^{-1}) and then cervical dislocation, and their hearts were swiftly excised from the thoracic cavity. A Langendorff perfusion device was utilized for retrograde perfusion with Ca^{2+}-free Tyrode's solution for approximately 5 min. Subsequently, Tyrode's solution containing 50 μmol·L^{-1} Ca^{2+} and collagenase was perfused for about 5 min to facilitate cardiac digestion. The ventricles were then trimmed and sheared in Tyrode's solution containing 200 μmol·L^{-1} $CaCl_2$. A gradient of Ca^{2+} solution ranging from 12.5 μmol·L^{-1} to 900 μmol·L^{-1} was progressively added to obtain single resting well-streaked ventricular myocytes without apparent damage. The isolated AMVMs were cultured in confocal dishes containing M199 medium (Gibco, USA). The AMVMs were then subjected to the following conditions for 48 h : Con, ISO (0.1 μmol·L^{-1}) group, ISO

Table 2 Primers sequences RT–PCR analysis

	Forward primer 5′-3′	Reverse primer 5′-3′
ANP	CGTCTTGGCCTTTTGGCTTC	GGTGGTCTAGCAGGTTCTTGAAA
BNP	GGAGAACACGGCATCATTGC	CTCCAGCAGCTTCTGCATCT
MYH6	TGCACTACGGAAACATGAAGTT	CGATGGAATAGTACACTTGCTGT
MYH7	ACTGTCAACACTAAGAGGGTCA	TTGGATGATTTGATCTTCCAGGG
18S	GTAACCCGTTGAACCCATT	CCATCCAATCGGTAGTAGCG

(0.1 μmol·L^{-1}) + LGZG (10^{-6} g·mL^{-1}), and ISO (0.1 μmol·L^{-1}) + atenolol (1 μmol·L^{-1}).

2.6. Real-time polymerase chain reaction (PCR)

Total ribonucleic acid (RNA) was extracted from frozen mouse left ventricular tissue or NMVMs using TRIzol Reagent (Beyotime, Shanghai, China). The extracted RNA was then reverse-transcribed into cDNA and analyzed *via* real-time PCR, following the manufacturer's protocol (Takara, Japan). The relative expression levels of target genes were quantified using the $2^{-\Delta\Delta Ct}$ method, with 18S serving as a reference gene. The primer sequences utilized in this study are presented in Table 2.

2.7. Western blotting and antibodies

Protein extraction from the hearts was performed using cold lysis buffer. The protein lysates were separated on 8%–12% SDS–PAGE gels and subsequently transferred to polyvinylidene difluoride or nitrocellulose membranes (Millipore, MA, USA). Following blockage with 5% skimmed milk, the membranes were incubated overnight at 4 °C with the following antibodies: anti-phospho-cyclic adenosine monophosphate (cAMP)-response element binding protein (CREB) (Ser133) (Cell Signaling Technology, MA, USA), anti-CREB (48H2) (Cell Signaling Technology, MA, USA), anti-PKA RI-α/β (Cell Signaling Technology, MA, USA), anti-PKAα/β/γ cat (B-4) (Santa Cruz, MA, USA), anti-CBP (Santa Cruz, MA, USA), anti-P300 (Santa Cruz, MA, USA), anti-natriuretic peptide A (ANP) (Abcam, Cambridge, CB, UK), anti-B-type natriuretic peptide (BNP) (Abcam, Cambridge, CB, UK), anti-lamin B1 (1 : 3000; Proteintech, Rosemont, IL, USA), and anti-glyceraldehyde 3-phosphate dehydrogenase (1 : 5000; Proteintech, Rosemont, IL, USA). The next day, the membranes were incubated with the appropriate secondary antibody for 90 min at 22–25 °C. Signal detection was performed using FluorChem E (Protein Simple, CA, USA), in accordance with the manufacturer's instructions.

Protein expression in NMVMs was analyzed using capillary Western blotting (Wes, Protein Simple, San Jose, CA, USA). The cells were lysed with radioimmunoprecipitation assay buffer (as previously described). Following protein concentration quantification, 0.4 μg of total protein was transferred to 12–230 kDa Separation Modules (Protein Simple) for separation. The antibodies were utilized as previously described. Analysis was conducted using the Compass for SW software (Bio-Techne, USA) to determine relative protein expression based on the area under the peak of the chemiluminescence chromatogram.

2.8. Immunofluorescence

AMVMs or NMVMs were fixed, permeabilized, and blocked with 5% bovine serum albumin for one hour. After a single phosphate-buffered saline wash, the cells were incubated with primary antibodies overnight at 4 °C. The primary antibodies utilized were: anti-phospho-CREB (Ser133) (1 : 100), anti-CBP (1 : 100), anti-P300 (1 : 100), anti-PKA RI-α/β (1 : 100), and anti-PKAα/β/γ cat (B-4) (1 : 50). Subsequently, the cells were incubated with Alexa Fluor 594-conjugated goat anti-mouse (1 : 200, AS054; Abclonal, Wuhan, China) or Alexa Fluor 488-conjugated goat anti-rabbit (1 : 200, AS053; Abclonal, Wuhan, China) secondary antibodies. Finally, the cell nuclei were stained with 4,6-diamidino-2-phenylindole (1 : 1 000, Beyotime, Beijing, China).

2.9. Enzyme-linked immunosorbent assay (ELISA)

The concentrations of cAMP and levels of PKA activity in heart tissue and adult rat cardiac myocytes were quantified using an ELISA kit, following the manufacturer's protocol (MEIMIAN Inc., Jiangsu, China).

2.10. AMVM Ca^{2+} transients

AMVMs were loaded with Fluo 4/am and F-127 (1 μmol·L^{-1}, Invitrogen, USA) for 10 min and allowed to settle in a chamber coated with laminin (10 mg·L^{-1}; Invitrogen, USA). The calcium transients were subsequently evaluated under a steady-state external field.

2.11. Measurement of cardiomyocyte sarcomere length

The AMVM sarcomere length was measured according to previously established methods [19]. The cells underwent incubation in NT buffer for 3 min before being photographed using a high-sensitivity digital CMOS camera (C11440-36 U, Hamamatsu Photonics K.K., Japan). Subsequently, the contraction amplitude was analyzed utilizing the ImageJ plug-in (National Institutes of Health, USA).

2.12. CREB-luciferase assays

To measure CREB transcription, a dual-luciferase reporter gene assay was conducted. NMVMs were seeded in 96-well plates at a density of 7000 cells·well^{-1} one day prior to transfection. Subsequently, the cells were cotransfected with plasmids encoding the luciferase reporter genes CREB-Luc and pGMLR-TK (Yeasen, Shanghai, China). Following an 8-hour incubation period, the cells were exposed to ISO or LGZG for 48 hours. The luciferase assay was performed using a dual-luciferase reporter gene assay kit (Yeasen, Shanghai, China), in accordance with the manufacturer's protocol.

2.13. Statistical analyses

All values are expressed as means ± standard error. Statistical analyses and graph generation were performed using GraphPad Prism version 8 (GraphPad, San Diego, CA, USA). Data comparisons were conducted using one-way analysis of variance followed by Tukey's post-hoc test. P values < 0.05 were deemed statistically significant.

3. Results

3.1. LGZG improves cardiac function in mice with ISO-induced CHF

C57BL/6J mice were administered ISO for 4 weeks concurrently with LGZG (from days 1 to 30) (Fig. 2A). Echocardiography was conducted weekly post-ISO administration to evaluate the effects of LGZG on cardiac function. Analysis of cardiac data revealed that the mice exhibited significantly increased interventricular septal thickness at end diastole, interventricular septal thickness at end systole (IVSs), left ventricular posterior wall thickness at end diastole (LVPWd), left ventricular posterior wall thickness at end systole (LVPWs), EF%, and FS% after

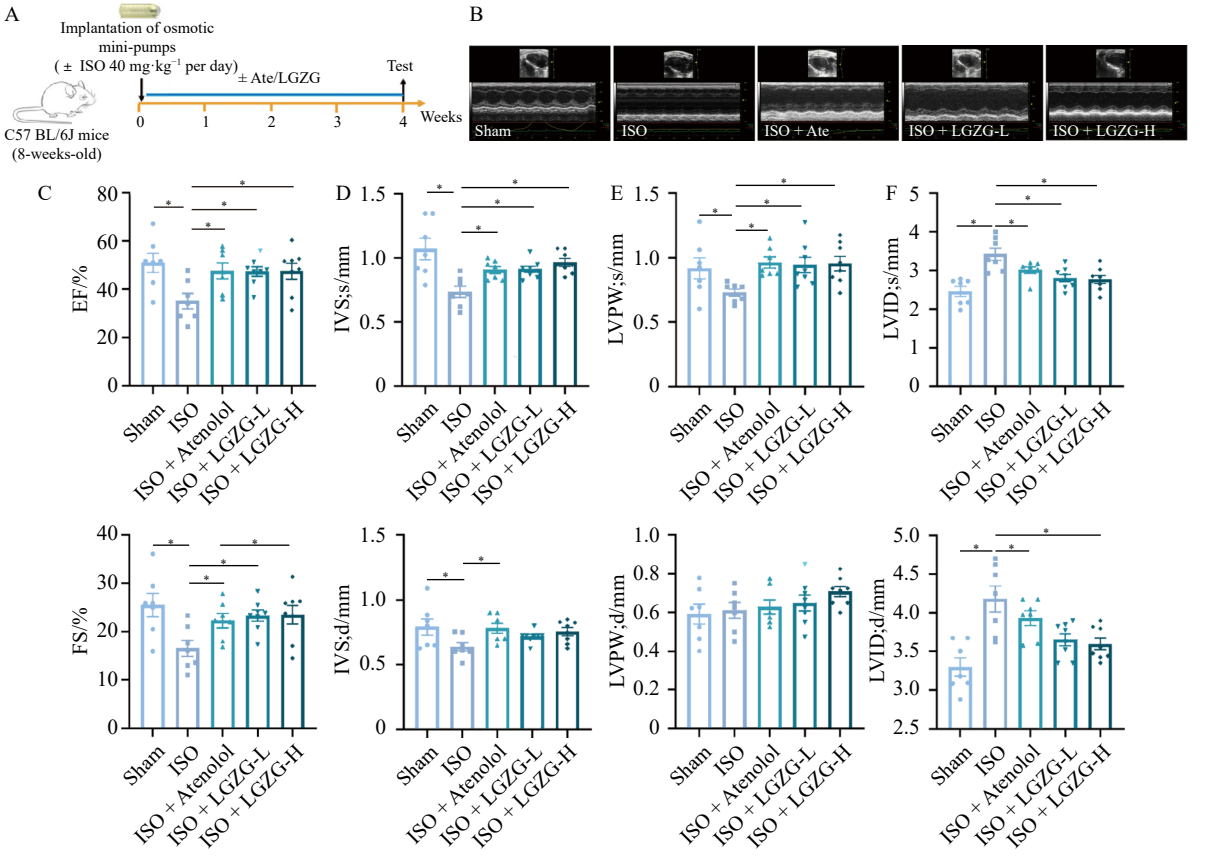

Fig. 2 LGZG improves cardiac function in mice with ISO-induced CHF. (A) Timeline graph of ISO action in mice. (B) Representative echocardiographic images at 4 weeks. (C–F) Quantification of echocardiogram parameters ($n \geq 6$). The data are expressed as means ± standard errors of the mean. $^{*}P < 0.05$. LGZG, Lingguizhugan decoction; ISO, isoproterenol; Ate, atenolol; CHF, chronic heart failure; EF, ejection fraction; FS, fractional shortening; LVEDs, left ventricular end-systolic diameter; LVEDd, left ventricular end-diastolic diameter; IVSd, interventricular septal thickness at end diastole; IVSs, interventricular septal thickness at end systole; LVPWd, left ventricular posterior wall thickness at end diastole; LVPWs, left ventricular posterior wall thickness at end systole.

1 week of ISO intervention, followed by gradual decreases over time. By the 4th week, IVSs, IVSd, LVPWs, EF%, and FS% were significantly lower in the ISO group compared to the sham group. Conversely, the trends in changes in left ventricular internal diameter at the end of diastole (LVIDd) and left ventricular internal diameter at the end of systolic (LVIDs) were reversed. At week 4, the left ventricular internal dimension was significantly enlarged (Figs. 2B–2F, S1). These findings indicate that cardiac morphology and function transitioned from a compensated to a decompensated state during ISO treatment. In contrast, LGZG mitigated cardiac dilatation and left ventricular dysfunction after 4 weeks of treatment, further decelerating CHF progression. No significant difference in cardiac function was observed between the 1.2 g·kg^{-1} and 2.4 g·kg^{-1} LGZG groups (Fig. 2).

3.2. LGZG reduces ISO-induced CHF in mice

Substantial increases in heart volume, lung volume, heart weight (HW) : tibial length (TL) ratio, lung weight (LW) : body weight (BW) ratio, and LW : TL ratio were observed in the ISO group (Figs. 3A, 3B). LGZG, particularly at high doses, mitigated ISO-induced increases in LW : BW and LW : TL ratios (Fig. 3B). Consistent results were obtained from macroscopic lung observations (Fig. 3A). Considering myocardial fibrosis as a crucial factor in cardiac remodeling, Masson and Sirius red staining were employed to identify cardiac collagen deposition. Histological findings revealed significantly higher interstitial and perivascular fibrosis in the ISO group compared to the sham group, while treatment with atenolol and LGZG notably suppressed ISO-induced cardiac fibrosis (Figs. 3C, 3D). To assess the effect of LGZG on biochemical markers of ISO-induced CHF, Western blotting assays and qRT-PCR analyses were conducted to detect the expression of ANP, BNP, and β-myosin heavy chain (β-MHC)/α-MHC in heart tissue from each group. LGZG reduced the protein and messenger RNA (mRNA) expression of ANP, BNP, and β-MHC/α-MHC in ISO-induced mice to levels comparable to those in the positive control group (Figs. 3E–3G).

3.3. Mechanisms by which LGZG improves ISO-induced CHF in mice

To further elucidate the mechanism by which LGZG ameliorates ISO-induced CHF in mice, we employed ELISA to measure cAMP content and PKA activity in each group, and quantified proteins extracted from mouse heart tissues. Western blotting was utilized to assess the expression of proteins associated with the Gs/PKA/CREB signaling pathway. LGZG attenuated the ISO-induced increase in cAMP content and overactivation of PKA (Figs. 4A, 4B) and suppressed the expression of PKARI, PKA cat, phosphorylated (p)-CREB, and CREB-binding proteins CBP and P300 (Figs. 4C–4E). Additionally, protein expression related to the G protein-coupled receptor kinase (GRK)/β-arrestin signaling pathway was analyzed *via* Western blotting. LGZG enhanced the protein expression of β1-AR and β-arrestin2 while inhibiting the protein expression of β-arrestin1, GRK2, GRK3, and GRK5 (Figs. 4F–4K). Consequently, the mechanism by which LGZG ameliorates ISO-induced CHF in mice may be attributed to the inhibition of Gs/PKA/CREB signaling pathway overactivation and GRK-/β-arrestin-mediated desensitization and internalization effects of β1 receptor.

3.4. Effects of LGZG on CHF in ISO-treated primary cardiomyocytes

Initially, we examined the impact of LGZG on ISO-treated AMVMs and NMVMs. ISO induced surface area hypertrophy in both AMVMs and NMVMs, which was mitigated by the administration

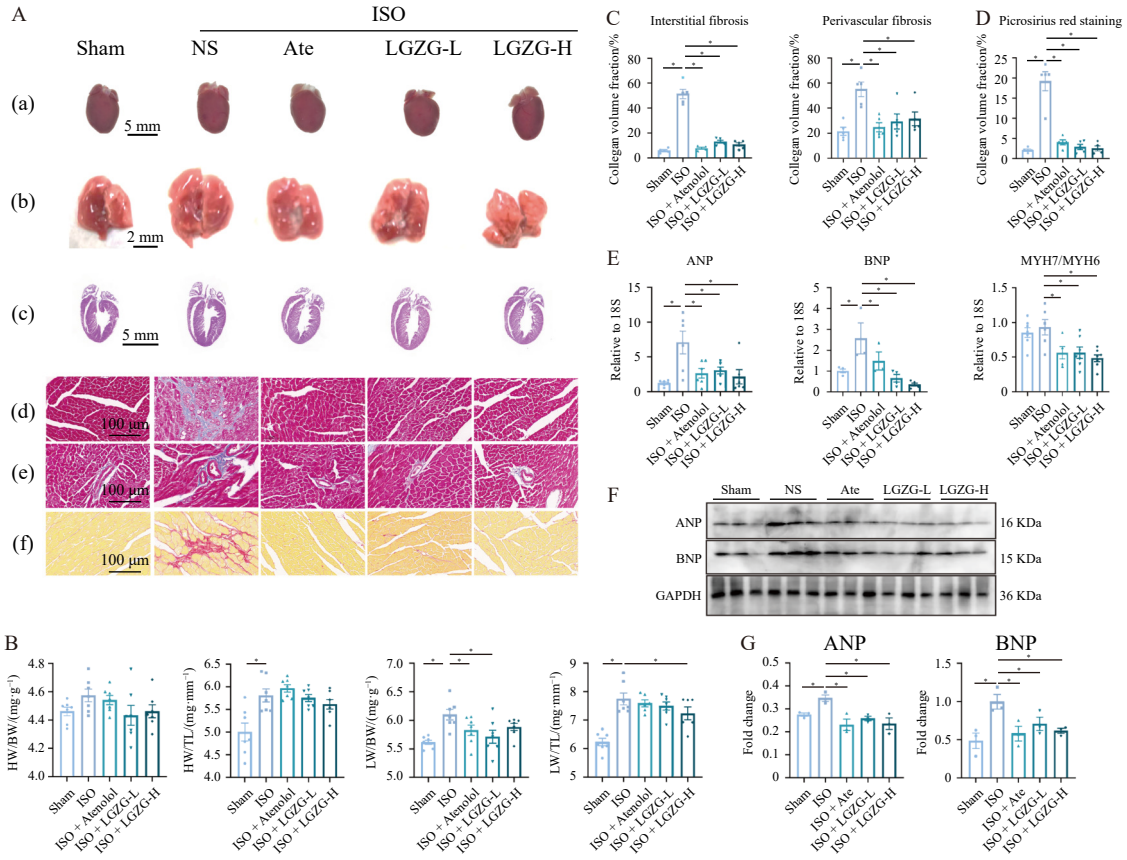

Fig. 3 LGZG attenuates CHF induced by ISO in mice. (A) Cardiac images: (a, b) Comparison of heart and lung sizes in mice receiving sham, ISO only, ISO + Ate (10 mg·kg^{-1}), ISO + LGZG (1.2 g·kg^{-1}), and ISO + LGZG (2.4 g·kg^{-1}) treatments. (c) Representative H&E staining overall. (d–f) Collagen deposition in 6-μm-thick heart sections was determined using Masson and Sirius red staining. (B) HW : BW, HW : TL, LW : BW, and LW : TL ratios ($n \geq 6$). (C, D) Quantifying cardiac interstitial fibrosis in each group ($n = 6$). (E) qRT-PCR analysis of ANP, BNP, and β-MHC/α-MHC mRNA normalized to 18S mRNA levels ($n \geq 3$). (F, G) Western blotting of ANP and BNP for each group ($n = 3$). The data are expressed as means ± standard errors of the mean. $^{*}P < 0.05$. LGZG, Lingguizhugan Decoction; CHF, chronic heart failure; ISO, isoproterenol; H&E, hematoxylin and eosin; ANP, anti-natriuretic peptide A; BNP, B-type natriuretic peptide; β-MHC, β-myosin heavy chain; α-MHC, α-myosin heavy chain; HW, heart weight; BW, body weight; LW, lung weight; TL, tibial length.

of LGZG and atenolol (Figs. 5A–5D). LGZG significantly suppressed the mRNA expression of ANP, BNP, and β-MHC/α-MHC in NMVMs exposed to ISO for 48 h, aligning with the effect of atenolol (Figs. 5E–5G). Subsequently, we explored the effects of LGZG on excitation-contraction coupling in AMVMs. Both LGZG and atenolol significantly enhanced the ISO-induced sarcomere contraction rate and amplitude of Ca^{2+} transient in AMVMs and extended their time to peak (TTP) and relaxation time constant (Tau) by 30%, thereby enhancing excitation-contraction coupling in AMVMs (Figs.5H–5L).

3.5. LGZG treatment modifies ISO-induced cAMP/PKA expression and activity in ventricular myocytes

To examine whether LGZG's reversal of ISO-induced CHF is associated with the activation of the Gs/PKA/CREB signaling pathway, we initially assessed cAMP content and PKA activity levels in cardiomyocytes. Both parameters were significantly elevated in the ISO group, while LGZG and atenolol mitigated the excessive increase in cAMP and the overactivation of PKA (Fig. 6A, 6B). Furthermore, LGZG and atenolol reduced the protein expression of PKARI and the PKA cat in ISO-treated cardiomyocytes (Figs. 6C–6E).

3.6. LGZG treatment modulates cAMP/PKA/CREB signaling in ISO-induced ventricular myocytes

PKA cat translocation to the nucleus induces CREB phosphorylation, which regulates transcription. Phosphorylation of the Ser133B site in CREB's N-terminal kinase-inducible domain activates CREB transcriptionally, enabling its binding to the transcriptional coactivator CBP/P300 to initiate target gene transcription. Consequently, we examined LGZG's impact on p-CREB and its transcription-binding protein, P300/CBP. Western blotting analysis revealed that both LGZG and atenolol suppressed the expression of p-CREB (Ser133) and the CREB-binding protein CBP/P300 in ISO-treated cardiomyocytes (Figs 6F, 6G). To further elucidate LGZG's effect on CREB transcriptional activity, NMVMs were transfected with a p-CREB luciferase reporter plasmid. While CREB transcriptional activity was elevated in the ISO group, LGZG treatment mitigated this increase in response to ISO stimulation ($P = 0.07$) (Fig. 6H). Similarly, atenolol significantly inhibited CREB transcription. Given that p-CREB (Ser133) and CBP/P300 interact to mediate gene transcription, we assessed their colocalization in NMVMs and AMVMs using immunofluorescence. The results demonstrated the presence of both p-CREB and CBP/P300 in the cells, with LGZG and atenolol significantly reducing p-CREB and CBP/P300 colocalization in the nucleus compared to the ISO group (Fig. S2).

3.7. LGZG treatment inhibits GRK-/β-arrestin1-mediated β1-AR desensitization effects and upregulate the expression of β-arrestin2 in ISO-induced ventricular myocytes

Loss of function in the β1-receptor signaling pathway and reduced responsiveness to catecholamines, leading to decreased cardiac variable force reserve, are major pathological changes in CHF. LGZG and atenolol upregulated the protein expression of β1-AR and β-arrestin2 while inhibiting the protein expression of β-arrestin1. β-ARK, a key molecule mediating the phosphorylation

and decoupling of β1-AR and regulating its function, prompted further examination of β-ARK-related molecules. Western blotting results revealed that LGZG and atenolol inhibited the expression of GRK2, GRK3, and GRK5 in ISO-treated cardiomyocytes (Figs. 6I–6L). To further investigate β-arrestin2's role in LGZG's cardioprotective effects, Barbadin, a β-arrestin2 inhibitor, was used for validation. The findings demonstrated that continuous ISO stimulation resulted in an enlargement of NMVM surface area

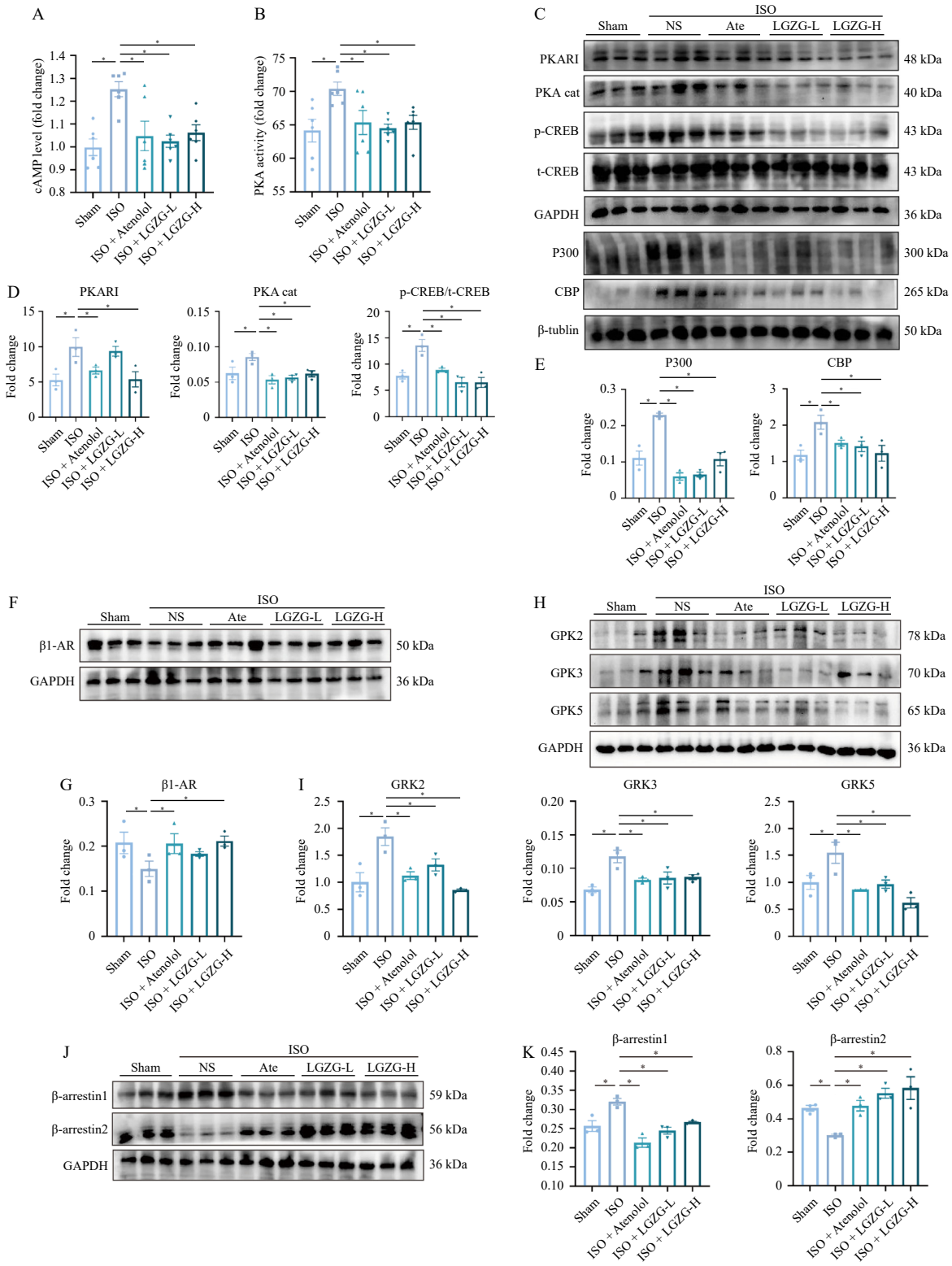

Fig. 4 Mechanisms by which LGZG improves ISO-induced CHF in mice. (A, B) ELISA for cAMP content and PKA activity in mice (n = 6). (C–E) Western blots showing the protein expression levels of PKARI, PKA cat, p-CREB, CBP, and P300 in each group (n = 3). (F, G) Western blots showing the protein expression levels of β1-AR(n = 3). (H, I) Western blots showing the protein expression levels of GRK2, GRK3, and GRK5 in each group (n = 3). (J, K) Western blots showing the protein expression levels of β-arrestin1 and β-arrestin2 in each group (n = 3). The data are expressed as means ± standard errors of the mean. $^{*}P < 0.05$. PKARI, PKA regulatory subunit-I; PKA cat, catalytic subunit; CREB, cAMP-response element binding protein; CBP/P300, CREB-binding protein; β1-AR, β1-adrenergic receptor; GRK2/3/5, G protein-linked receptor kinase 2/3/5; LGZG, Lingguizhugan decoction; ISO, isoproterenol; CHF, chronic heart failure; ELISA, enzyme-linked immunosorbent assay; cAMP, cyclic adenosine monophosphate; PKA, protein kinase A.

and a decrease in AMVM contractility. LGZG treatment significantly improved this pathological change, and its protective effect was partially abolished by subsequent Barbadin administration (Fig. S3).

4. Discussion

This study corroborates the cardioprotective effects of the classical TCM prescription LGZG both *in vivo* and *in vitro*. The findings demonstrate that LGZG primarily enhances cardiomyocyte contractile function and reverses pathological myocardial hypertrophy. Furthermore, preliminary research indicates that LGZG modulates β1-AR/Gs/β-arrestin signaling bias.

LGZG has been extensively utilized in various cardiovascular diseases due to its efficacy in invigorating heart yang, resolving qi, and facilitating water movement. Its clinical application has demonstrated remarkable effectiveness [20]. Building on these TCM theories and clinical evidence, this study focused on investigating the efficacy of LGZG in ISO-induced CHF and conducting a preliminary exploration of its mechanism of action. The findings indicate that LGZG significantly mitigated myocardial hypertrophy and left ventricular diastolic dysfunction induced by ISO. It also reduced the expression levels of hypertrophy-related genes, including ANP, BNP, and MHY7/MHY6. Furthermore, in vitro experiments demonstrated that LGZG inhibited the increase in surface area of both NMVMs and AMVMs. Cardiomyocyte contractility is known to be associated with an imbalance in calcium handling [21]. The present study suggests that LGZG can ameliorate both the weakening of cardiomyocyte sarcomere contraction induced by continuous ISO stimulation and the decrease in calcium transient, indicating that LGZG inhibits ISO-induced CHF.

The pathogenesis of CHF is intricate, with hyperactivation of the sympathetic nervous system, particularly β1-AR/Gs/cAMP/PKA signaling, playing a crucial role [22]. Recent studies have indicated that β-arrestin-mediated desensitization and internalization of β1-AR, leading to sustained inactivation, contribute significantly to adverse effects on the myocardium. These effects result in reduced myocardial contractility and metabolic disorders in cardiomyocytes, contributing to pathological CHF progression [23]. Furthermore, β-arrestin may function as a scaffold between β1-AR and multiple signaling pathways, including epidermal growth factor receptor (EGFR), extracellular signal-regulated kinase, and NF-κB [24, 25], which may be related to the cardioprotective effects of LGZG [13]. Consequently, β1-AR exhibits a bidirectional pathway coupled with G protein and β-arrestin, activating downstream signaling pathways to produce diverse, and sometimes opposing biological effects. This phenomenon, termed "biased activation" [26], is a focal point in CHF research [27]. The cardioprotective effects of LGZG have been associated with various signaling pathways such as AKT, AMPKs, JUN, and NF-κB [12–14]. These pathways are also integral components of downstream intracellular signaling pathways modulated by β-arrestin. Thus, it is hypothesized that the synergistic regulation of the β-AR/Gs/β-arrestin signaling deflection system by LGZG may be the primary mechanism underlying its anti-heart failure effect.

The primary mechanism of ISO-induced CHF involves the overactivation of the classical Gs/cAMP/PKA signaling pathway. CREB, a crucial intracellular nuclear transcription factor, intersects the cAMP signaling pathway with TNF and RAGE pathways that mediate oxidative stress, playing a pivotal role in CHF development [28]. In pathological conditions, cAMP binding to PKA releases the active catalytic subunit of PKA, which translocates to the nucleus, activating phosphorylated CREB expression and initiating transcription of downstream-related genes [29]. Our findings indicate that LGZG significantly mitigated the ISO-induced increase in cAMP content and overactivation of PKA activity in cells and mice, while inhibiting PKA protein expression. Furthermore, LGZG inhibited the nuclear translocation of PKA cat, as demonstrated by cellular immunofluorescence. Phosphorylation of the Ser133 site in CREB's *N*-terminal kinase-inducible domain leads

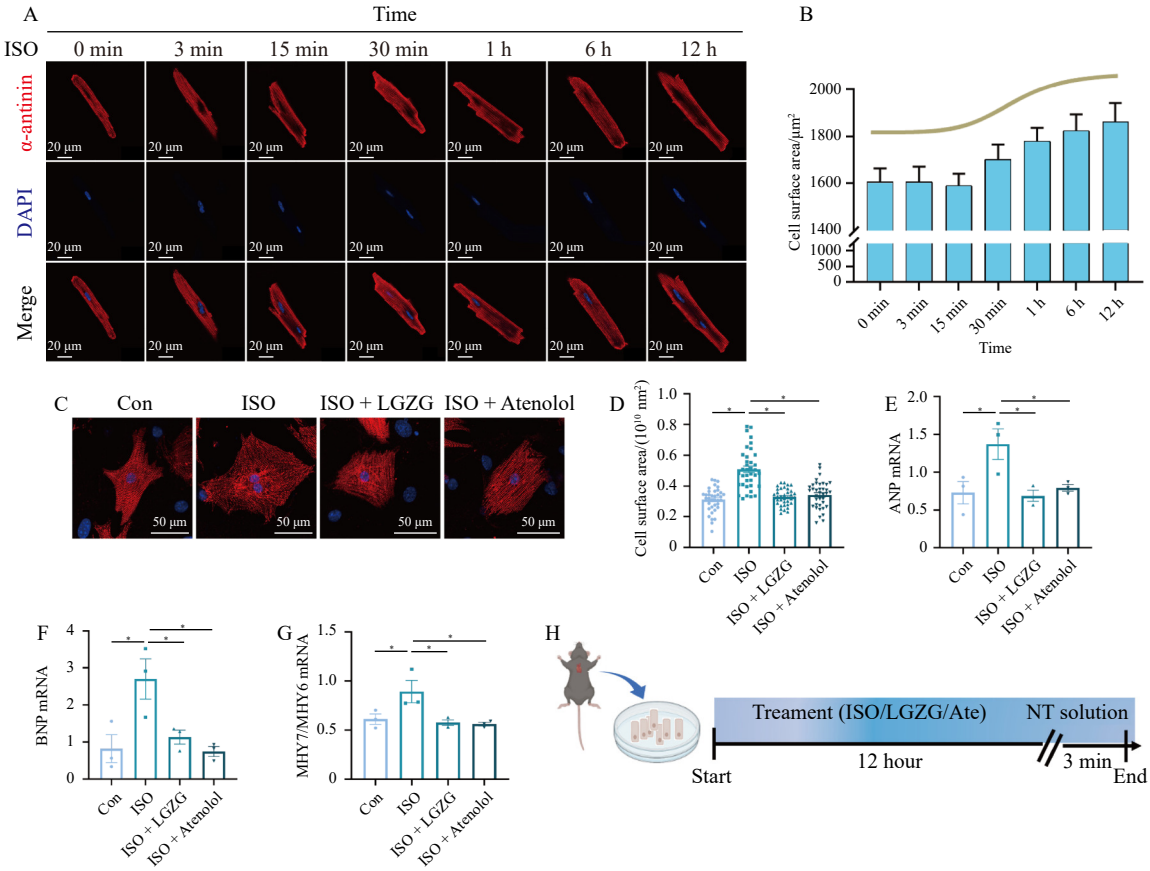

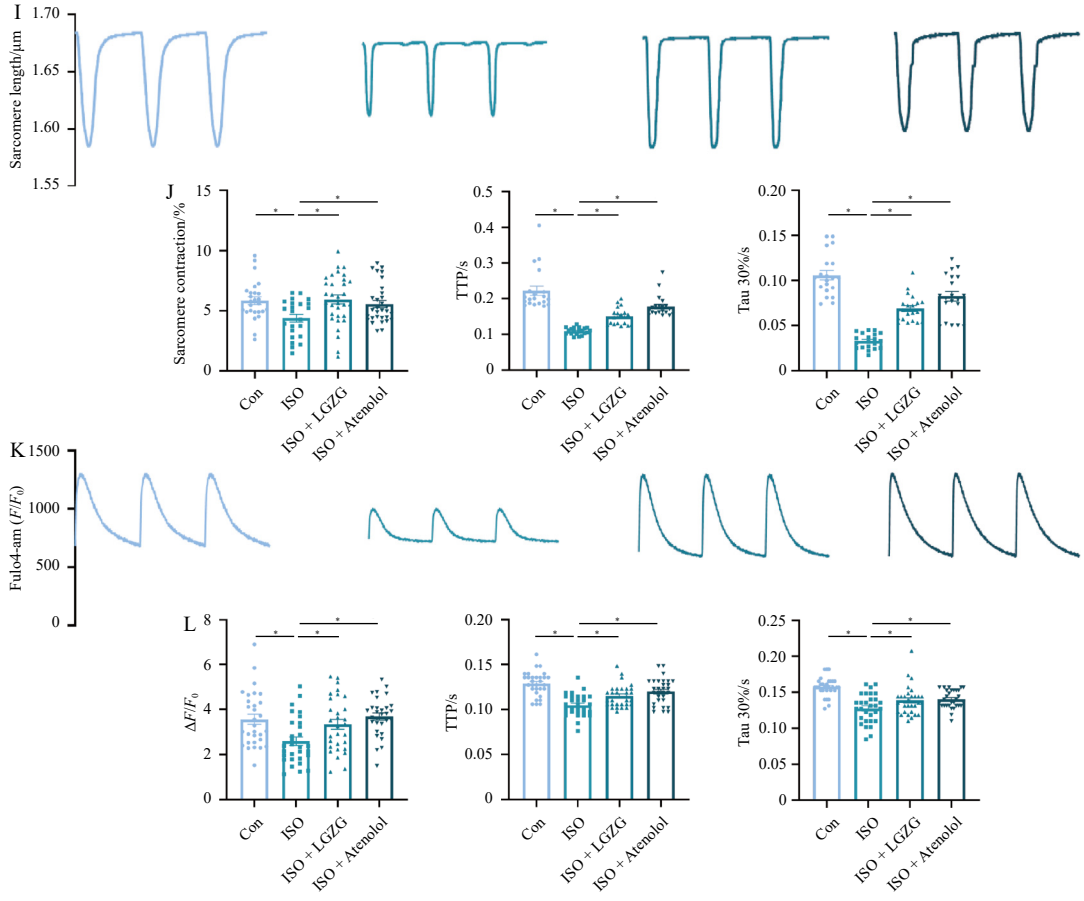

Fig. 5 Effect of LGZG on CHF in ISO-treated ventricular myocyte. (A, B) AMVMs were treated with ISO (0.1 μmol·L^{-1}) for 0 min, 3 min, 15 min, 30 min, 1 h, 6 h, and 12 h, and changes in surface area were observed by α-actin staining (≥ 50 cells per group from three independent experiments). (C, D) NMVMs were exposed to ISO (1 μmol·L^{-1}) and treated with LGZG (10^{-6} g·mL^{-1}) for 48 h, and their surface area was observed by applying α-actin staining (30 cells per group from three independent experiments). (E–G) qRT-PCR analysis of ANP, BNP, and β-MHC/α-MHC mRNA levels in each group normalized to 18S mRNA levels (n = 3). (H) Schematic representation of the processing of AMVMs for the detection of sarcomere contraction and Ca^{2+} transients. (I) Representative tracings of sarcomere contraction after stimulation with ISO (0.1 μmol·L^{-1}) in adult mouse cardiomyocytes for 12 h. (J) Quantification of sarcomere contraction (30 cells per group from three independent experiments). (K) Representative tracings of Ca^{2+} transients after stimulation with ISO in adult mouse cardiomyocytes for 12 h. (L) Quantification of Ca^{2+} transients (30 cells per group from three independent experiments). The data are expressed as means ± standard errors of the mean. $^{*}P < 0.05$ *vs* 0 min, Lingguizhugan Decoction; CHF, chronic heart failure; ISO, isoproterenol; β-MHC, β-myosin heavy chain; α-MHC, α-myosin heavy chain; AMVMs, adult mouse ventricular myocytes; NMVMs, neonatal mouse ventricular myocytes; ANP, atrial natriuretic peptide; BNP, B-type natriuretic peptide; TTP, time to peak; Tau 30%, sarcomere relaxation time constant 30%.

to its transcriptional activation. Once activated, CREB binds to the transcriptional coactivator CBP/P300, initiating target gene transcription [30]. In this study, p-CREB (Ser133) protein expression was significantly elevated in the ISO-induced CHF model, with upregulated protein transcriptional activity. Moreover, protein expression of the CREB transcriptional coactivator CBP/P300 was increased, as was the degree of CREB and CBP/P300 colocalization in the nucleus. These findings align with previous research results. Collectively, these observations suggest that LGZG inhibits β1-AR activation-mediated Gs/cAMP/PKA signaling, thereby modulating the subsequent CREB-mediated signaling pathway.

Another channel coupled with β1-AR is its interaction with β-arrestin, which facilitates β1-AR desensitization and internalization. Upon phosphorylation by GRKs, β1-AR recruits β-arrestin1 to form the β1-AR/GRK/β-arrestin complex, theoretically promoting the receptor's uncoupling from Gs to terminate the signal. The phosphorylated receptor is then internalized, forming an endosome that recycles directly to the plasma membrane *via* fast-recycling [29, 31, 32]. Our analysis of proteins associated with desensitization and internalization revealed that LGZG could reverse the upregulation of β-arrestin1 and GRK2/3/5 expression, consequently restoring β1-AR expression. Notably, β-arrestin2 exhibited an expression trend opposite to β-arrestin1, aligning with previous research that highlights the contrasting impacts of these proteins on mammalian myocardium. β-arrestin1 negatively affects cardiac function by mediating β1-AR desensitization and internalization, while β-arrestin2 demonstrates potential cardioprotective properties through mechanisms such as EGFR transactivation and SERCA2 SUMOylation [33, 34]. In this study, the application of the β-arrestin2-specific inhibitor Barbadin further validated the cardioprotective role of β-arrestin2, which represents one pathway through which LGZG improves CHF; however, the specific mechanism requires further investigation. LGZG partially inhibits β-arrestin1/GRK signaling-mediated β1-AR desensitization and internalization while upregulating β-arrestin2 expression to counteract CHF.

Our findings indicate that ISO facilitates the formation of GPCR/G/β-arrestin complexes, enabling bidirectional signaling. This observation appears to challenge previous conclusions suggesting that β1-AR signaling initiates with Gs protein activation and terminates through β-arrestin, with these pathways being mutually exclusive. The discrepancy may be attributed to the specific tail conformation adopted by GPCR, which allows simultaneous binding to G proteins and β-arrestin at the phosphorylated C-terminal tail [35]. Furthermore, β1-AR exhibits transient interactions with β-arrestin and rapidly recycles internalized receptors to the plasma membrane. In this process, β-arrestin can mediate the swift binding of Gβγ to Gα, reconstituting the G protein heterotrimer to initiate a new signaling cycle [36]. Additionally, substantial evidence supports intracellular signaling in internalized β1-AR and other GPCRs [37].

This study has certain limitations that warrant consideration.

Firstly, the signaling model of G proteins or β-arrestin following β1-AR activation in this research was relatively simplified. Further investigation is necessary to elucidate the activation of various GRKs and β-arrestin isoforms, as well as their downstream signaling pathways. Secondly, the impact of LGZG on β-arrestin-mediated cardioprotective signaling remains unclear. The preliminary results suggest a potential relationship with β-arrestin2-mediated EGFR transactivation and SERCA2A SUMOylation, but this hypothesis requires additional research for confirmation.

5. Conclusion

Both overactivation and inactivation of β1-AR play crucial roles in the pathogenesis of CHF, highlighting the essential nature of maintaining a balanced β1-AR activation state. Our experimental findings demonstrate that LGZG functions by inhibiting the persistent activation of β1-AR through the Gs/cAMP/PKA pathway and the desensitized internalization of β1-AR *via* GRKs/β-arrestin1, while simultaneously enhancing β-arrestin2

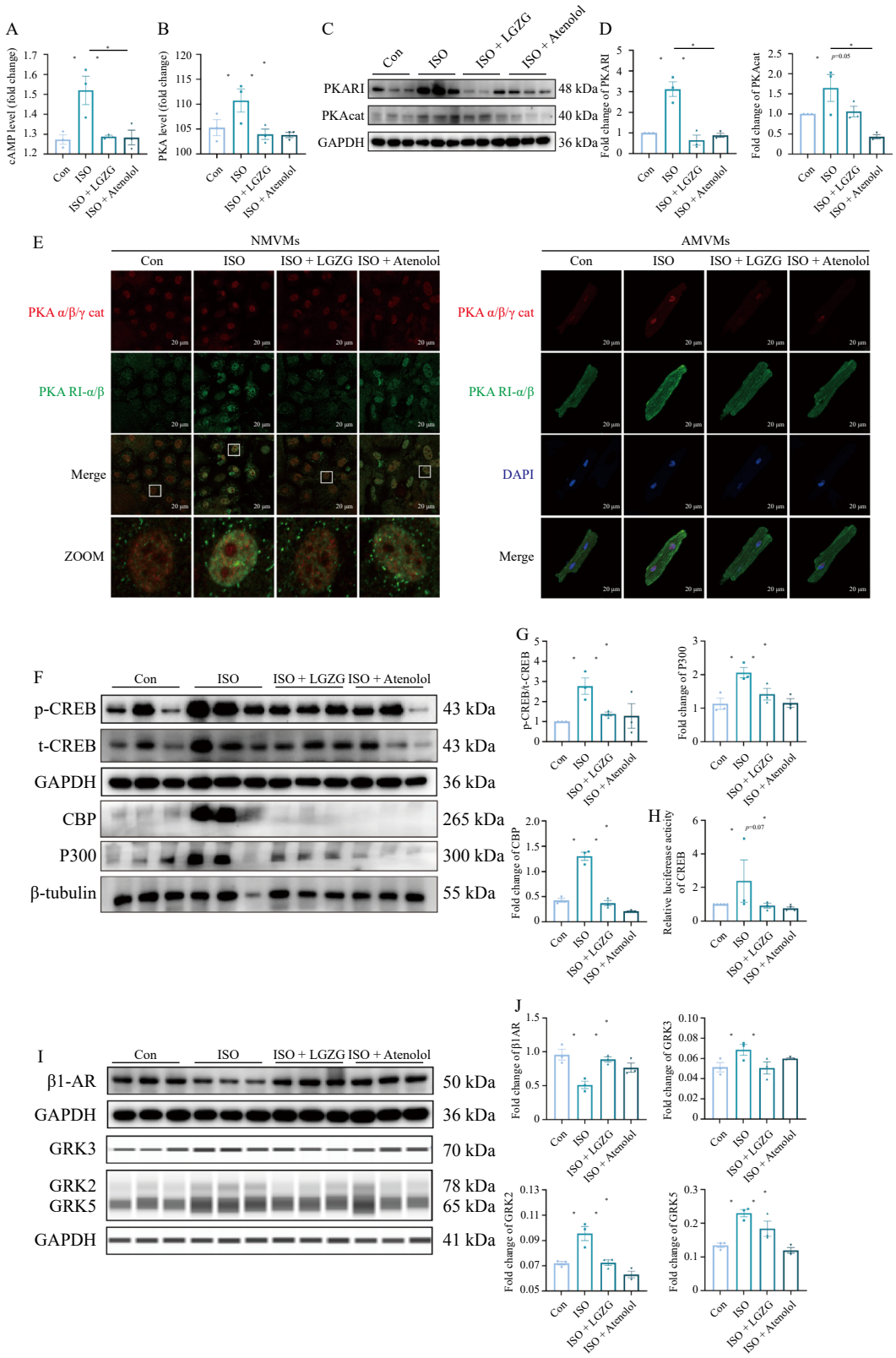

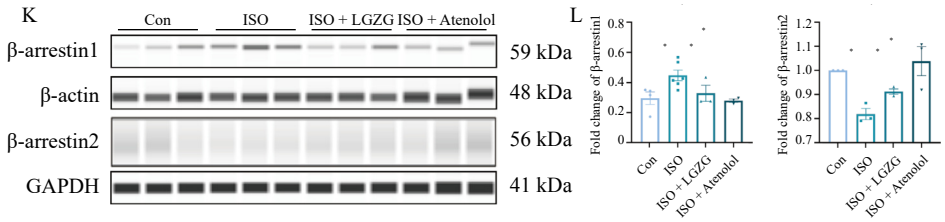

Fig. 6 LGZG treatment modulates synergistically β1-AR/Gs/GRKs/β-arrestin signaling bias in ventricular myocytes. (A, B) The cAMP content and PKA activity in NMVMs were measured using cAMP and PKA kits (n = 3). (C, D) Western blots showing the protein expression of PKARI and PKA cat in each group (n = 3). (E) Representative immunofluorescence images showing the altered distribution of PKARI and PKA cat in NMVMs and AMVMs in each group. (F, G) Western blots showing the expression of p-CREB/t-CREB, CBP, and P300 in each group of cells (n = 3). (H) CREB activity in NMVMs treated with ISO expressed as the ratio of CREB-Luc to Renilla luciferase. (I, J) Western blots showing the protein expression levels of β1-AR, GRK2, GRK3, and GRK5 in each group (n = 3). (K, L) Western blots showing the protein expression levels of β-arrestin1 and β-arrestin2 in each group (n = 3). The data are expressed as means ± standard errors of the mean. $^{*}P < 0.05$. LGZG, Lingguizhugan decoction; ISO, isoproterenol; cAMP, cyclic adenosine monophosphate; PKA, protein kinase A; NMVMs, neonatal mouse ventricular myocytes; PKARI, PKA regulatory subunit-I; PKA cat, catalytic subunit; p-CREB, phospho-cyclic adenosine monophosphate-response element binding protein; t-CREB, total cyclic adenosine monophosphate-response element binding protein; CBP, cyclic adenosine monophosphate-response element-binding protein-binding protein; GRK, G protein-coupled receptor kinase; β1-AR, β1-adrenergic receptor; ISO, isoproterenol.

expression. These results suggest that LGZG may alleviate CHF by precisely regulating β1-AR activation and synergistically modulating β1-AR/Gs/GRKs/β-arrestin signaling bias, thereby ensuring beneficial signaling while preventing overstimulation (Fig. 7). This evidence provides an experimental foundation for the clinical application of LGZG.

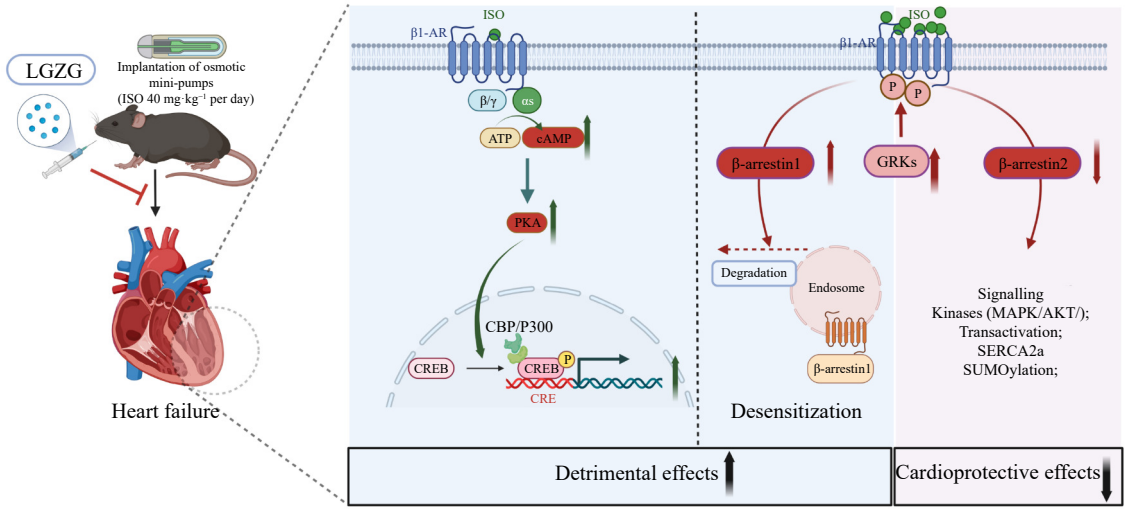

Fig. 7 Schematic representation of the effect of LGZG on β1-adrenergic receptor/Gs/β-arrestin signaling bias. ISO, isoproterenol; LGZG, lingguizhugan granule; PKARI, PKA regulatory subunit-I; PKAcat, catalytic subunit; CREB, cAMP-response element binding protein; CBP, CREB-Binding Protein; β1-AR, β1-adrenergic receptor; GRK, G protein-coupled receptor kinase.

Funding

This work was supported by the National Natural Science Foundation of China (No. 82074054), Shanghai Municipal Commission of Health and Family Planning (No. ZY (2021-2023)-0208), Youth Program of the National Natural Science Foundation of China (No. 81903831), Shanghai Municipality: Shanghai Chenguang Program (No. 19CG48)， and Natural Science Foundation of Shanghai（No.24ZR1465900).

Declarations of competing interest

The authors declare that the research was conducted in the absence of any commercial or financial relationships that could be construed as potential conflicts of interest.

References

1 Kamel R, Leroy J, Vandecasteele G, et al. Cyclic nucleotide phosphodiesterases as therapeutic targets in cardiac hypertrophy and heart failure. *Nat Rev Cardiol*. 2023;20(2):90-108. https://doi.org/10.1038/s41569-022-00756-z.
2 Heidenreich PA, Bozkurt B, Aguilar D, et al. 2022 AHA/ACC/HFSA guideline for the management of heart failure: executive summary: a report of the American college of cardiology/American heart association joint committee on clinical practice guidelines. *Circulation*. 2022;145(18):e876-e894. https://doi.org/10.1161/CIR.0000000000001062.
3 de Lucia C, Eguchi A, Koch WJ. New insights in cardiac β-adrenergic signaling during heart failure and aging. *Front Pharmacol*. 2018;9(AUG):904. https://doi.org/10.3389/fphar.2018.00904.
4 Gurevich VV, Gurevich EV. Biased GPCR signaling: possible mechanisms and inherent limitations. *Pharmacol Ther*. 2020;211:107540. https://doi.org/10.1016/j.pharmthera.2020.107540.
5 Wisler JW, Xiao K, Thomsen ARB, et al. Recent developments in biased agonism. *Curr Opin Cell Biol*. 2014;27(1):18-24. https://doi.org/10.1016/j.ceb.2013.10.008.
6 Cahill TJ, Thomsen ARB, Tarrasch JT, et al. Distinct conformations of GPCR-β-arrestin complexes mediate desensitization, signaling, and endocytosis. *Proc Natl Acad Sci U S A*. 2017;114(10):2562-2567. https://doi.org/10.1073/pnas.1701529114.
7 Hao P, Jiang F, Cheng J, et al. Traditional Chinese medicine for cardiovascular disease: evidence and potential mechanisms. *J Am Coll Cardiol*. 2017;69(24):2952-2966. https://doi.org/10.1016/j.jacc.2017.04.041.
8 Ji B, Zhao Y, Yu P, et al. LC-ESI-MS/MS method for simultaneous determination of eleven bioactive compounds in rat plasma after oral administration of Ling-Gui-Zhu-Gan Decoction and its application to a pharmacokinetics study. *Talanta*. 2018;190:450-459. https://doi.org/10.1016/j.talanta.2018.08.020.
9 Sun S, Xun G, Zhang J, et al. An integrated approach for investigating pharmacodynamic material basis of Lingguizhugan Decoction in the treatment of heart failure. *J Ethnopharmacol*. 2022;295:115366. https://doi.org/10.1016/j.jep.2022.115366.
10 Wang X, Gao Y, Tian Y, et al. Integrative serum metabolomics and network analysis on mechanisms exploration of Ling-Gui-Zhu-Gan Decoction on doxorubicin-induced heart failure mice. *J Ethnopharmacol*. 2020;250:112397. https://doi.org/10.1016/j.jep.2019.112397.
11 Wu CX, Liu Y, Zhang JC. Chronic intermittent hypoxia and hypertension: a review of systemic inflammation and Chinese medicine. *Chin J Integr Med*.

2013;19(5):394-400. https://doi.org/10.1007/s11655-013-1459-x.
12 Wang X, Gao Y, Zhang J, et al. Revealment study on the regulation of lipid metabolism by Lingguizhugan Decoction in heart failure treatment based on integrated lipidomics and proteomics. *Biomed Pharmacother*. 2023;158: 114066. https://doi.org/10.1016/j.biopha.2022.114066.
13 Chen Y, Li L, Hu C, et al. Lingguizhugan Decoction dynamically regulates MAPKs and AKT signaling pathways to retrogress the pathological progression of cardiac hypertrophy to heart failure. *Phytomedicine.* 2022;98: 153951. https://doi.org/10.1016/j.phymed.2022.153951.
14 Shi Y, Liu C, Xiong S, et al. Ling-Gui-Qi-Hua Formula alleviates left ventricular myocardial fibrosis in rats with heart failure with preserved ejection fraction by blocking the transforming growth factor-β1/Smads signaling pathway. *J Ethnopharmacol*. 2023;317:116849. https://doi.org/10.1016/j.jep.2023.116849.
15 Li X, Xu G, Wei S, et al. Lingguizhugan Decoction attenuates doxorubicin-induced heart failure in rats by improving TT-SR microstructural remodeling. *BMC Complement Altern Med*. 2019;19(1):360. https://doi.org/10.1186/s12906-019-2771-6.
16 Wang J, Gareri C, Rockman HA. G-protein-coupled receptors in heart disease. *Circ Res*. 2018;123(6):716-735. https://doi.org/10.1161/CIRCRESAHA.118.311403.
17 Hu P, Guo S, Yang S, et al. Stachytine hydrochloride improves cardiac function in mice with ISO-induced heart failure by inhibiting the α-1, 6-fucosylation on *N*-glycosylation of β1AR. *Front Pharmacol*. 2022;12:834192. https://doi.org/10.3389/fphar.2021.834192.
18 Zheng J, Tian J, Wang S, et al. Stachydrine hydrochloride suppresses phenylephrine-induced pathological cardiac hypertrophy by inhibiting the calcineurin/nuclear factor of activated T-cell signalling pathway. *Eur J Pharmacol*. 2020;883:173386. https://doi.org/10.1016/j.ejphar.2020.173386.
19 Pasqualin C, Gannier F, Yu A, et al. SarcOptiM for imageJ: high-frequency online sarcomere length computing on stimulated cardiomyocytes. *Am J Physiol Cell Physiol*. 2016;311(2):C277-C283. https://doi.org/10.1152/ajpcell.00094.2016.
20 Xu J, Wang R, You S, et al. Traditional Chinese medicine Lingguizhugan Decoction treating non-alcoholic fatty liver disease with spleen-yang deficiency pattern: study protocol for a multicenter randomized controlled trial. *Trials*. 2020;21(1):512. https://doi.org/10.1186/s13063-020-04362-7.
21 Xue G, Li D, Wang Z, et al. Interleukin-17 upregulation participates in the pathogenesis of heart failure in mice *via* NF-κB-dependent suppression of SERCA2a and Cav1.2 expression. *Acta Pharmacol Sin*. 2021;42(11):1780-1789. https://doi.org/10.1038/s41401-020-00580-6.
22 Hartupee J, Mann DL. Neurohormonal activation in heart failure with reduced ejection fraction. *Nat Rev Cardiol*. 2017;14(1):30-38. https://doi.org/10.1038/nrcardio.2016.163.
23 Mahmood A, Ahmed K, Zhang Y. β-Adrenergic receptor desensitization/down-regulation in heart failure: a friend or foe? *Front Cardiovasc Med*. 2022;9:925692. https://doi.org/10.3389/fcvm.2022.925692.
24 Tilley DG, Kim IM, Patel PA, et al. beta-Arrestin mediates beta1-adrenergic receptor-epidermal growth factor receptor interaction and downstream signaling. *J Biol Chem*. 2009;284(30):20375-20386. https://doi.org/10.1074/jbc.M109.005793.
25 Sun S, Cao H, Yao N, et al. β-Arrestin 2 mediates arginine vasopressin-induced IL-6 induction *via* the ERK1/2-NF-κB signal pathway in murine hearts. *Acta Pharmacol Sin*. 2020;41(2):198-207. https://doi.org/10.1038/s41401-019-0292-y.
26 Shao SY, Sun MH, Ma XJ, et al.Novel phenanthrene/bibenzyl trimers from the tubers of Bletilla striata attenuate neuroinflammation via inhibition of NF-κB signaling pathway. *Chin J Nat Med*. 2024;22:441-454. https://doi.org/10.1016/S1875-5364(24)60641-2.
27 Liu X, Ma L, Li HH, et al. β-Arrestin-biased signaling mediates memory reconsolidation. *Proc Natl Acad Sci U S A*. 2015;112(14):4483-4488. https://doi.org/10.1073/pnas.1421758112.
28 Zhou H, Li N, Yuan Y, et al. Activating transcription factor 3 in cardiovascular diseases: a potential therapeutic target. *Basic Res Cardiol*. 2018;113(5):37. https://doi.org/10.1007/s00395-018-0698-6.
29 Serio S, Pagiatakis C, Musolino E, et al. Cardiac aging is promoted by pseudohypoxia increasing p300-induced glycolysis. *Circ Res*. 2023;133(8): 687-703. https://doi.org/10.1161/CIRCRESAHA.123.322676.
30 Bektik E, Sun Y, Dennis AT, et al. Inhibition of CREB-CBP signaling improves fibroblast plasticity for direct cardiac reprogramming. *Cells*. 2021;10(7): 1572. https://doi.org/10.3390/cells10071572.
31 Sato PY, Chuprun JK, Schwartz M, et al. The evolving impact of g protein-coupled receptor kinases in cardiac health and disease. *Physiol Rev*. 2015;95 (2):377-404. https://doi.org/10.1152/physrev.00015.2014.
32 Seyedabadi M, Gharghabi M, Gurevich EV, et al. Structural basis of GPCR coupling to distinct signal transducers: implications for biased signaling. *Trends Biochem Sci*. 2022;47(7):570-581. https://doi.org/10.1016/j.tibs.2022.03.009.
33 Zhang LS, Wang YJ, Ju YY, et al. Role for engagement of β-arrestin2 by the transactivated EGFR in agonist-specific regulation of δ receptor activation of ERK1/2. *Br J Pharmacol*. 2015;172(20):4847-4863. https://doi.org/10.1111/bph.13254.
34 Liu Z, Liu X, Liu L, et al. SUMO1 regulates post-infarct cardiac repair based on cellular heterogeneity. *J Pharm Anal*. 2023;13(2):170-186. https://doi.org/10.1016/j.jpha.2022.11.010.
35 Nguyen AH, Thomsen ARB, Cahill TJ, et al. Structure of an endosomal signaling GPCR-G protein-β-arrestin megacomplex. *Nat Struct Mol Biol*. 2019;26(12):1123-1131. https://doi.org/10.1038/s41594-019-0330-y.
36 Thomsen ARB, Plouffe B, Cahill TJ, et al. GPCR-G protein-β-arrestin super-complex mediates sustained G protein signaling. *Cell*. 2016;166(4):907-919. https://doi.org/10.1016/j.cell.2016.07.004.
37 Irannejad R, Tomshine JC, Tomshine JR, et al. Conformational biosensors reveal GPCR signalling from endosomes. *Nature*. 2013;495(7442):534-538. https://doi.org/10.1038/nature12000.